Molecular Structure, Vibrational Spectroscopic, Electronic Properties and Chemical Stability of *p-n*-Alkylbenzoic Acids (*n*BAC) — a Comparison Using DFT and HF Methods

S. Prasad and D.P. Ojha*

School of Physics, Sambalpur University, Jyoti Vihar-768 019, Sambalpur, Odisha, India

(Received March 10, 2018)

The molecular structure and vibrational spectra of homologous series of nematogenic *p-n*-alkylbenzoic acids (*n*BAC) with 4 (4BAC), 5 (5BAC), 6 (6BAC), 7 (7BAC), 8 (8BAC) and 9 (9BAC) carbon atoms in the alkyl chain have been investigated using the density functional Becke3–Lee–Yang–Parr (B3LYP) level with the basis set 6-31++G(d.p) and the Hartree–Fock with the same basis set. The computations have been carried out for all the molecules but detailed results have been reported only for 9BAC molecule. However, the salient features of others have also been reported. The observed vibrational spectra have been resolved and assigned in detail for comparison with the molecules. These results indicate that DFT and HF values are slightly different at both the levels. A comparison of electronic properties such as HOMO (E_{HOMO}), LUMO (E_{LUMO}) energies, energy gap (E_g), ionization potential (I), electron affinity (A), electro negativity (χ), chemical hardness (η), electronic chemical potential (μ), electrophilicity index (ω), and softness (S) has been made. It has been observed that the substitution of additional alkyl group has a profound control on energy band gap, and the conductivity of molecules.

DOI: 10.12693/APhysPolA.134.557

PACS/topics: vibrational spectra, nematogens, DFT and HF methods

1. Introduction

A central problem in modeling of new and advanced materials, particularly complex molecules such as liquid crystals (LCs), understands the relation between molecular structure and material properties [1]. The quest for new materials, whether driven by their potential for applications or simply by natural scientific curiosity about structure/phase stability relationship, has always been a vital part of the LC scenario. Indeed, the fundamental research in this direction opened many doors to provide effective solutions to the different problems [2, 3]. The applications of LCs have unquestionably added incentive to the quest for designing new materials with superior properties such as transition temperatures, phase behavior, and stability [4].

Further, the benzoic acids and their salts are permitted food preservatives in many types of foods [5]. Substituted benzoic acids are very important materials in chemical and pharmaceutical industries and can be prepared by oxidation of the corresponding substituted toluenes [6–8]. A recent patent reported that their activity was related to novel synergistic compositions that selectively control on tumor tissue [9].

The vibrational spectroscopy deals with a double averaging of information. The first averaging is due to the fact that for most samples the observed molecules are randomly oriented (such as gas, liquid, amorphous or polycrystalline solids), the second is due to using unpolarized radiation, so that the orientation of the observed transition moment relative to the propagation direction of probing beam is not revealed [10].

In view of this, the vibrational spectroscopy has become the informative tool in order to the analysis of intensity and position changes of vibrational bands that makes it possible to identify the liquid crystal phases and calculate the orientational order parameters. We can also obtain information about the tail and core orientational order by observing the band corresponding to vibrations of the relevant functional group [11]. Further, an understanding of physics and chemistry of organic compounds requires the conception of molecular orbital properties and spectra. These spectroscopic and structural features are a big challenge to the interplay between theory and experiment. The main difficulties hindering a reliable computational approach is related to the size of such systems and the presence of strong electron correlation effects. Both properties are difficult to treat in the framework of quantum mechanical methods in the Hartree–Fock (HF) theory. The method based on density functional theory (DFT) applied to small and middle sized system provides rather good accuracy at low computational cost [12, 13].

In the present article, the calculation of molecular structures and vibrational spectra (with IR and Raman intensity) of nematogens, namely; 4BAC, 5BAC, 6BAC, 7BAC, 8BAC and 9BAC molecules have been discussed using the DFT incorporated with the basis set B3LYP/6-31++G (d.p) and HF theory with the same basis set but detailed results have been reported only for 9BAC molecule. However, the salient features of other

*corresponding author; e-mail: durga_ojha@hotmail.com

molecules have also been reported. Further, the electronic properties such as HOMO, LUMO energies, energy gap, ionization energy, electron affinity, electronegativity, chemical hardness, electronic chemical potential, electrophilicity index, and softness have been reported. An attempt has been made to discuss the effect of an increment in the alkyl chains on the isolated molecules.

2. Computational details

2.1. Quantum chemical calculations

The quantum chemical calculations have been performed at the density functional B3LYP and HF levels of theory supplemented with standard 6-31++G (d.p) basis set at the Gaussian 09 program to calculate bond length, bond angles and vibrational frequencies with the IR intensities and the Raman scattering activities. The 6-31++G (d.p) split valence-shell basis set was augmented by *d* polarization function on heavy atoms and *p* polarization function on hydrogen atoms have been used [14, 15]. To reproduce the Raman spectra, Gaussian calculated activities have converted in corresponding Raman intensities using the empirical relation of the Raman scattering theory [16, 17]. The structural and electronic properties of all the molecules have been investigated and compared with each other.

3. Results and discussion

3.1. Molecular structure

The DFT optimized molecular structure of *n*BAC has been shown in Fig. 1a–f. As evident from Table I, the total energy of nematogens exhibit the following order (magnitude wise):

9BAC > 8BAC > 7BAC > 6BAC > 5BAC > 4BAC.

TABLE I

Total energy of 4BAC, 5BAC, 6BAC, 7BAC, 8BAC and 9BAC molecules.

Molecule	Energy [AU]
4BAC	−578.12871941
5BAC	−617.44573990
6BAC	−656.75877871
7BAC	−696.08043108
8BAC	−735.39897188
9BAC	−774.71638388

Much of the interesting phenomenology of liquid crystals involves in the geometry and dynamics of the structure. Hence Fig. 1a–f is essential to understand and design the new molecules. Optimized bond lengths, bond angles and dihedral angles at the DFT/B3LYP/6-31++G (d.p) level and HF/6-31++G (d.p) level of molecules have been given in Table II. The DFT and HF values are slightly different as HF calculation does not include electron–electron interaction term. Therefore, we have discussed

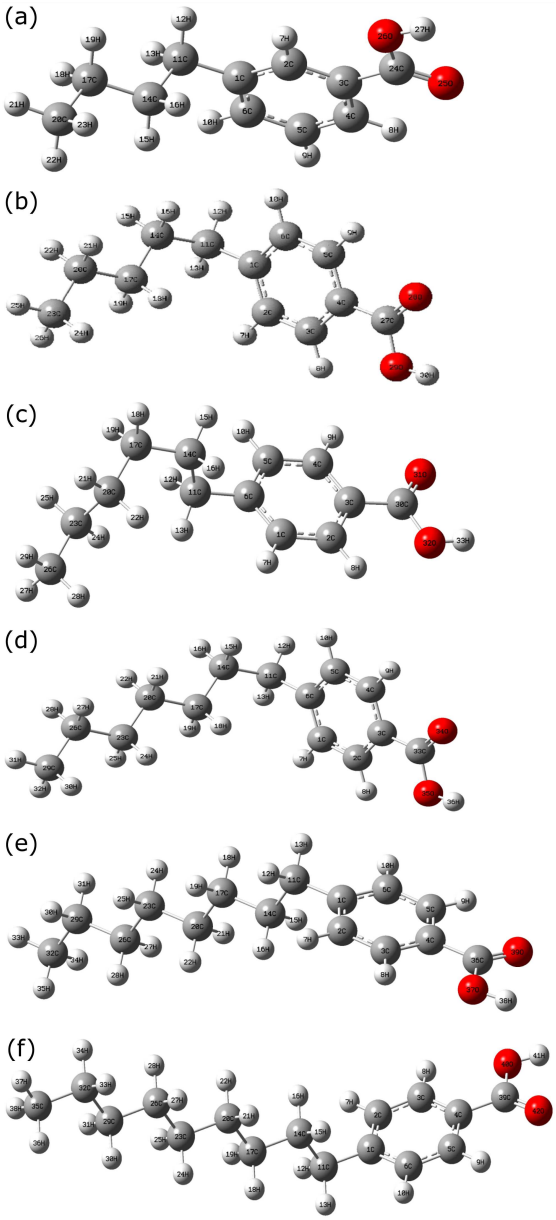

Fig. 1. Optimized electronic structure of 4BAC, 5BAC, 6BAC, 7BAC, 8BAC and 9BAC molecules using the DFT method.

only the DFT results. Evidently, the bond length of C39-O42 and C39-O40 have shorter values for 9BAC molecule while those length of C11-C14, C14-C17, C17-C20, C20-C23, C23-C26, C26-C29 and C29-C32 respectively have found to be larger. These geometrical parameters are sensitive to the hydrogen bonding.

Taking into account, the above consideration, the computed data (Table II) are slightly different at both the level (DFT and HF) theories. Also, angle α (C4-C39-O42) has been found to be larger while angle α (C1-C11-C14) has shorter value for 9BAC molecule. The same trend has been observed for other molecules. These discrepancies may be due to intra-molecular hydrogen bonding.

TABLE II

Optimized geometrical parameters of 9BAC molecules using DFT and HF methods

9BAC	DFT	HF	9BAC	DFT	HF
Bond lengths [Å]			Bond angles [°]		
C1-C2	1.404	1.392	C1-C2-C3	121.19	121.02
C2-C3	1.393	1.384	C2-C3-C4	119.96	120.02
C3-C4	1.403	1.390	C3-C4-C5	119.39	119.44
C4-C5	1.402	1.391	C4-C5-C6	120.13	120.16
C5-C6	1.392	1.382	C5-C6-C1	121.09	120.93
C6-C1	1.404	1.393	C6-C1-C2	118.21	118.40
C1-C11	1.512	1.512	C1-C11-C14	112.99	112.91
C11-C14	1.543	1.536	C11-C14-C17	113.07	112.74
C14-C17	1.534	1.529	C14-C17-C20	113.36	113.17
C17-C20	1.534	1.529	C17-C20-C23	113.61	113.30
C20-C23	1.534	1.529	C20-C23-C26	113.56	113.32
C23-C26	1.534	1.529	C23-C26-C29	113.67	113.35
C26-C29	1.534	1.529	C26-C29-C32	113.65	113.40
C29-C32	1.534	1.529	C29-C32-C35	113.33	113.09
C32-C35	1.533	1.528	C6-C1-C11	120.85	120.75
C4-C39	1.483	1.484	C2-C1-C11	120.90	120.82
C39-O40	1.361	1.330	C5-C4-C39	118.35	118.42
C39-O42	1.217	1.192	C3-C4-C39	122.25	122.12
			C4-C39-O40	113.30	113.68
			C4-C39-O42	125.17	124.64
			O40-C39-O42	121.52	121.66

3.2. Vibrational spectra

The harmonic-vibrational frequencies calculated for 9BAC molecule at the B3LYP level using the double valence basis set along with diffuse and polarization functions, 6-31++G (d.p) have been given in Table III.

TABLE III

Calculated vibrational frequencies [cm^{-1}] of 9BAC using the DFT/B3LYP/6-31++G(d.p) level

Wavenumber	Intensity		Assignment (PEDs)
	IR	Raman	
3769	103.55	169.34	rOH
3223	1.87	104.99	Arom rCH
3216	2.29	85.67	Arom rCH
3179	10.67	81.20	Arom rCH
3178	14.30	66.85	Arom rCH
3100	46.28	116.91	Arom rCH
3095	73.49	35.78	Arom rCH
3082	79.96	10.61	rCH_2 asymmetric
3067	121.12	15.63	rCH_2 asymmetric
3060	5.26	2.25	rCH_2 asymmetric
3053	0.03	63.51	rCH_2 asymmetric
3042	1.00	0.53	rCH_2 asymmetric
3034	80.01	61.67	rCH_2 asymmetric
3032	0.97	71.74	rCH_2 asymmetric
3029	50.81	193.34	rCH_2 asymmetric
3027	0.11	15.87	rCH_2 asymmetric
3024	0.107	234.86	rCH_2 asymmetric
3019	95.75	21.48	rCH_2 symmetric
3014	26.43	94.10	rCH_2 symmetric
3007	0.05	1.91	rCH_2 symmetric
3005	2.37	366.15	rCH_2 symmetric
3002	0.54	9.67	rCH_2 symmetric
3001	1.29	13.79	rCH_2 symmetric
1786	434.97	176.02	rCO
1657	87.51	276.35	Arom rCC+ Arom φ_a(CCC)
1614	7.36	4.05	Arom rCC
1546	2.67	1.14	Arom rCC
1517	12.90	0.44	Arom rCC+ ρCH_2
1513	0.01	0.26	Arom rCC+ ρCH_2
1508	2.05	3.25	ρCH_2
1502	7.79	8.91	CH_3ipr
1501	0.24	1.03	ρCH_2
1495	1.35	30.49	ρCH_2
1492	0.24	73.09	ρCH_2
1491	0.06	6.30	ρCH_2
1488	0.14	1.01	ρCH_2
1450	19.51	2.81	Arom rCC+βOH+ ρCH_2
1417	2.21	0.68	CH_3sb
1406	0.59	0.17	ωCH_2
1405	0.15	0.69	ωCH_2
1395	0.97	7.35	βOH+ωCH_2
1377	0.29	26.22	ωCH_2
1371	140.08	23.70	βCH+rCO+βOH+ ωCH_2
1363	39.77	6.45	βCH+rCO+ τCH_2
1349	1.57	18.77	ωCH_2
1342	1.90	0.52	βCH
1338	0.78	0.89	τCH_2
1336	0.05	0.02	τCH_2
1327	0.22	1.85	τCH_2
1323	0.17	35.42	rCO+τCH_2
1313	0.23	6.55	ωCH_2
1309	0.27	6.30	τCH_2+μCH_2
1279	0.06	0.48	τCH_2+μCH_2
1272	0.88	2.89	ωCH_2
1242	0.07	1.12	τCH_2+μCH_2+ βCH
1230	0.22	10.05	ωCH_2+βCH
1227	0.90	23.02	ωCH_2+βCH+ Arom φ_a(CCC)+rCC2
1216	47.48	12.52	βCH+τCH_2
1210	0.01	1.57	τCH_2+rCO
1190	219.73	78.35	βCH+rCC1
1146	2.17	2.43	βCH+τCH_2
1137	6.85	35.05	βCH+φ_{c2}(CCC)+ CH_3ipb

TABLE III cont.

TABLE III cont.

Wavenumber	Intensity		Assignment (PEDs)
	IR	Raman	
1112	105.98	2.61	βCH+Arom φ_a(CCC)
1096	64.04	0.77	βCH+τCH_2
1073	2.89	42.32	φ_{c2}(CCC)
1065	0.07	9.82	ωCH_2
1064	0.29	6.72	ωCH_2
1054	1.85	5.18	rCC2
1035	9.21	0.10	Arom φ_a(CCC)+τCH_2
1034	7.10	0.22	Arom φ_a(CCC)+τCH_2 +rCC2
1027	0.35	4.39	φ_{c2}(CCC)
1001	2.09	4.39	γCH+φ_{c2}(CCC)
997	0.46	0.57	γCH
990	0.37	0.92	γCH+rCC2
985	0.88	1.26	γCH
968	0.08	0.16	γOH+μCH_2+ τCH_2
896	0.99	6.62	φ_{c2}(CCC)+CH_3ipb
895	0.45	0.22	μCH_2
872	14.53	2.93	γCH+γCC1
859	0.33	0.31	γCH
838	1.58	27.89	γCH+rCC2+ Arom φ_a(CCC)
828	0.09	0.15	μCH_2
782	35.18	6.82	γCH+γCC1+ γOH+Arom φ_a(CCC)
774	0.25	0.03	μCH_2
744	0.64	0.03	μCH_2
742	41.00	4.10	γCH
733	0.01	0.00	μCH_2
732	4.59	0.01	μCH_2
715	39.23	1.14	μCH_2+γCH
650	0.55	6.69	Arom φ_a(CCC)
621	32.38	0.75	γOH+Arom φ_a(CCC)+ φ_{c1}(OCO)
594	51.87	1.86	γOH
531	35.93	1.42	γOH+γCH+γCC2
505	6.24	0.62	τCC1+τCC2
487	2.71	0.05	φ_{c2}(CCC)
459	5.40	0.16	γCH+γOH+φ_{c2}(CCC)
416	0.38	0.01	γCH
402	5.60	2.58	φ_{c2}(CCC)
365	1.04	0.29	φ_{c2}(CCC)+γCH+ γOH
349	0.44	0.16	μCH_2
315	0.98	1.76	φ_{c2}(CCC)
275	0.02	0.59	φ_{c2}(CCC)
205	0.04	2.12	φ_{c2}(CCC)
193	1.30	0.14	τCC1
162	0.01	0.00	μCH_2
151	0.02	1.56	φ_{c2}(CCC)

r = stretching, τ = twisting, ω = wagging, β = in-plane bending, μ = rocking, γ = out of plane bending, ρ = scissoring, ipr = in-plane rocking, ips = in-plane stretching, ipb = in-plane bending, opb = out of plane bending, sb = symmetric bending, φ_a = aromatic angle bending, φ_c = chain angle bending

A comparison of the calculated frequencies reveal the overestimation of the values due to neglect of anharmonicity in real system. However, inclusion of electron correlation in density functional theory to a certain extent makes the frequency value smaller. Reduction in the computed harmonic vibrations, through basis is sensitive only marginal as observed in the DFT values using 6-31++G (d.p). Any way not withstand the level of calculations, it is customary to scale down the calculated harmonic frequencies. The potential distributions (PEDs) have been also calculated. The assignments were shown in Table III. The present PEDs reveal that the most of the normal modes are superposition of several different vibrations. Hence, it is a little difficult to assign a normal mode of a particular stretching or bending vibration. The calculated IR and the Raman spectra of 9BAC molecule have been presented in Fig. 2.

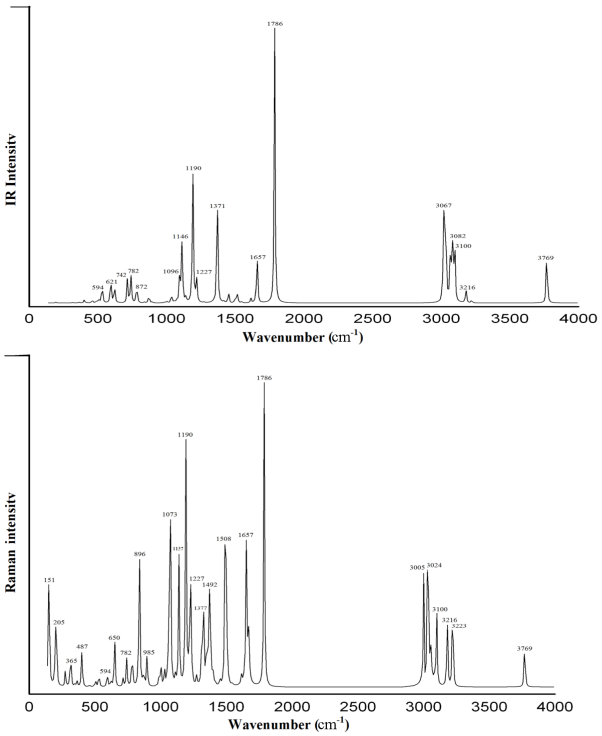

Fig. 2. Theoretical IR and Raman spectra of 9BAC molecules using the DFT method.

3.2.1. Vibrational frequencies in the range of 4000–1500 cm^{-1}

In the vibrational spectra, the strength of hydrogen bond determines the position of O–H bond. Evidently, a very strong absorption peak has been observed at 3769 cm^{-1}, due to O–H stretching vibration in 9BAC molecule. The aromatic structure shows the presence of C–H stretching vibration in the region 3100–3000 cm^{-1}, which is the characteristic region for the identification of C–H stretching vibration [18]. The asymmetric CH_2 stretching vibrations are generally observed in the region of 3100–3000 cm^{-1}, while symmetric CH_2 stretching vibrations are generally observed between 3000 and

2900 cm^{-1} [17]. Evidently, for 9BAC molecule, the asymmetric CH_2 stretching vibrations have observed at 3082 and 3067 cm^{-1} while symmetric CH_2stretching vibrations observed at 3019 and 3022 cm^{-1}, respectively.

The C–C aromatic stretch known as semi-circle stretching has been observed at 1657 cm^{-1} coupled with other vibrations. The other C–H stretching vibration has also been found in the spectra with appropriate PED. Furthermore, CH_2 scissoring vibrations have been observed for the molecule, namely 9BAC.

3.2.2. Vibrational frequencies in the range of 1500–1000 cm^{-1}

There are four strong modes of vibrations for 9BAC molecule, namely in-plane bending-β(CH) coupled with other modes of vibration at frequency 1371 cm^{-1}, in-plane bending-β(CH) coupled with other modes of vibration at frequencies 1190, 1146, and 1096 cm^{-1}, respectively.

3.2.3. Vibrational frequencies below 1000 cm^{-1}

There are five frequencies assigned for 9BAC molecule, frequencies 872, 782 cm^{-1} correspond to out of plane bending $-\gamma$(CH) coupled with other modes of vibration, frequency 742 cm^{-1} corresponds to out of plane bending $-\gamma$(CH), frequency 621 cm^{-1} corresponds to out of plane bending $-\gamma$(OH) coupled with other modes of vibration and frequency 594 cm^{-1} corresponds to out of plane bending $-\gamma$(OH), respectively.

4. Electronic properties

The HOMO and LUMO studies are very important for quantum chemistry. These orbitals are also known by the name frontier orbitals, because they lie at the outermost boundaries of electron in the molecules. Both the HOMO and LUMO are the main orbitals that take part in the chemical stability [19]. The HOMO, LUMO energies, and energy gap (E_g) of lower and higher homologous series, namely 4BAC and 9BAC molecules are shown in Fig. 3a,b. The energy of the HOMO is directly related to the ionization energy, LUMO energy is directly related to the electron affinity. The energy gap (E_g) between the HOMO and LUMO is an important factor in the determination of molecular transport properties and photo stability. The chemical hardness is a measure for resistance to deformation or change, is very important tool to study the stability of molecular systems, and is also an approximation to the first electron excitation energy. The lowering of energy separation between the HOMO and LUMO clearly explicates the charge transfer interactions taking place within the molecules. The average value of the HOMO and LUMO energies is related to the electronegativity. The negative of the electronegativity is the chemical potential. Evidently, the 4BAC molecule exhibits lower band gap; hence its electron conductivity is high (Fig. 3a,b). Lower the value of energy gap explains the eventual charge transfer interactions taking place within the molecule. The calculated values of electronic properties of isolated molecules, namely; 4BAC, 5BAC, 6BAC, 7BAC, 8BAC and 9BAC have been given in Table IV for comparison.

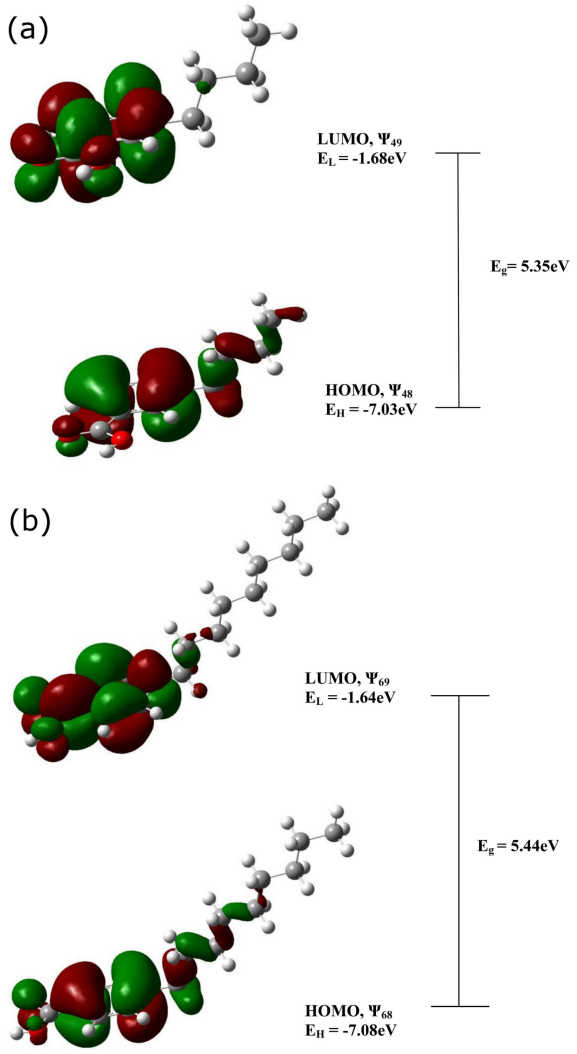

Fig. 3. HOMO and LUMO pattern of lower and higher homologous series, namely (a) 4BAC and (b) 9BAC.

TABLE IV

Calculated values of ionization potential $I = (-E_{\mathrm{HOMO}})$, electron affinity $A = (-E_{\mathrm{LUMO}})$, electronegativity $\chi = (I + A)/2$, chemical hardness $\eta = (I - A)/2$, chemical potential $\mu = -(I + A)/2$, electrophilicity index $\omega = \mu^2/2\eta$, and softness $S = 1/2\eta$

Molecule	I	A [eV]	χ [eV]	η [eV]	μ [eV]	ω [eV]	S [eV^{-1}]
	[eV]						
4BAC	7.03	1.68	4.35	2.67	−4.35	3.54	0.19
5BAC	7.11	1.66	4.38	2.72	−4.38	3.52	0.18
6BAC	7.09	1.64	4.36	2.72	−4.36	3.49	0.18
7BAC	7.10	1.66	4.38	2.72	−4.38	3.52	0.18
8BAC	7.09	1.64	4.36	2.72	−4.36	3.49	0.18
9BAC	7.08	1.64	4.36	2.72	−4.36	3.49	0.18

5. Global reactivity descriptors

A molecule having ionization potential I or electron affinity A loses or admits an electron hardly [20, 21]. By the Koopmans approximation [22, 23], the ionization potential and electron affinity of any molecule can be calculated using the relations

$$I = -E_{\mathrm{HOMO}},$$

$$A = -E_{\mathrm{LUMO}}.$$

The Koopmans theorem for closed-shell molecules [23] results in the hardness of the molecule

$$\eta = (I - A)/2.$$

The chemical potential of the molecule

$$\mu = -(I + A)/2.$$

The softness of the molecules

$$S = 1/2\eta.$$

The electronegativity of the molecule

$$\chi = (I + A)/2.$$

The electrophilicity index of the molecule

$$\omega = \mu^2 S.$$

Using the above relations the electronic properties of 4BAC, 5BAC, 6BAC, 7BAC, 8BAC and 9BAC molecules have been listed in Table IV.

6. Effect of alkyl chain length on chemical stability

The majority of mesogenic molecules are composed of an aromatic core, to which one or two alkyl chains are attached. The primary role of alkyl chains is to widen the liquid crystal range. The liquid crystal properties, such as the nematic-isotropic transition temperature and the entropy of transition, are also influenced by the presence of alkyl chain [24]. Evidently, a comparison between lower and higher homologous series, namely 4BAC and 9BAC of molecules shows a clear preference for an increment in homologue number to exhibit HOMO and LUMO energies (Fig. 3a and b). Moreover, the energy gap ($E_{\mathrm{LUMO}} - E_{\mathrm{HOMO}}$) also shows the same preference. This provides valuable information regarding enhancing the stability of liquid crystal materials.

7. Conclusions

The present computation leads to the following conclusions:

1. A very strong absorption peak has been observed at 3769 cm^{-1}, due to O–H stretching vibration in 9BAC molecule.

2. The angle α (C4-C39-O42) has found to be larger while angle α (C1-C11-C14) has shorter value for 9BAC molecule. The same trend has also been observed for all the molecules. These discrepancies may be due to intra-molecular hydrogen bonding.

3. The substitution of additional alkyl group has a profound control on band gap, and the conductivity of molecules.

4. The DFT and HF values are slightly different as HF calculation does not include electron–electron interaction term.

5. A comparison of the calculated frequencies indicates the overestimation of the values due to neglect of anharmonicity in real system. However, inclusion of electron correlation in density functional theory to a certain extent makes the frequency value smaller.

Acknowledgments

One of the authors, namely Ms. Seema Prasad, is thankful to the UGC, New Delhi, India for providing the financial support in the form of JRF under the RGNF scheme.

References

[1] Y.S. Prakash, P.K. Kumar, M.A. Kumar, T.P. Kumar, M. Rajiv, *Phys. Scr.* **83**, 1 (2011).

[2] J.P.H. Ortiz, B.T. Gettelfinger, J. Razo, J.J.D. Pablo, *J. Chem. Phys.* **134**, 1 (2011).

[3] S.S. Sastry, T.V. Kumari, S.S. Begum, V.V. Rao, *Liq. Cryst.* **38**, 277 (2011).

[4] T. Araki, T. Buscaglia, T. Bellini, H. Tanaka, *Nature Mater.* **10**, 303 (2011).

[5] K. Kreutz, A. Schlossberg, U.S. Patent 6395, 720 B1, 2002.

[6] I.C. Khoo, S.T. Wu, *Optics and Non Linear Optics of Liquid Crystals*, World Sci., Singapore 1993.

[7] M.R. Wilson, *Chem. Soc. Rev.* **36**, 1881 (2007).

[8] P.L. Praveen, D.P. Ojha, *Phys. Rev. E* **83**, 051710 (2011).

[9] W. Koch, M.C. Holthansen, *A Chemist's Guide to Density Functional Theory*, Wiley-VCH, Weinheim 2000.

[10] J.A. Pollard, in: *Food Preservatives*, Eds. N.J. Russel, G.W. Gould, AVI Publ., New York 1991, p. 235.

[11] R.A. Sheldon, J.K. Kochi, *Metal-Catalyzed Oxidations of Organic Compounds*, Academic, New York 1981.

[12] M. Hudlicky, *Oxidation in Organic Chemistry*, ACS Monograph 186, American Chemical Society, Washington, DC 1990.

[13] B.M. Trost, *Comprehensive Organic Synthesis (Oxidation)*, Pergamon, New York 1991.

[14] V. Mukherjee, T. Yadav, *Spectrochim. Acta A* **165**, 167 (2016).

[15] M.J. Frisch, G.W. Trucks, H.B. Schlegel, G.E. Suzerain, M.A. Robb, J.R. Cheeseman Jr., J.A. Montgomery, T. Vreven, K.N. Kudin, J.C. Burant, J.M. Millam, S.S. Iyengar, J. Tomasi, V. Barone, B. Mennucci, M. Cossi, G. Scalmani, N. Rega, G.A. Petersson, H. Nakatsuji, M. Hada, M. Ehara, K. Toyota, R. Fukuda, J. Hasegawa, M. Ishida, T. Nakajima, Y. Honda, O. Kitao, H. Nakai, M. Klene, X. Li, J.E. Knox, H.P. Hratchian, J.B. Cross, V. Bakken, C. Adamo, J. Jaramillo, R. Gomperts, R.E. Stratmann, O. Yazyev, A.J. Austin, R. Cammi, C. Pomelli, J.W. Ochterski, P.Y. Ayala, K. Morokuma, G.A. Voth, P. Salvador, J.J. Dannenberg, V.G. Zakrzewski, S. Dapprich, A.D. Daniels, M.C. Strain, O. Farkas, D.K. Malick, A.D. Rabuck, K. Raghavachari, J.B. Foresman, J.V. Ortiz, Q. Cui, A.G. Baboul, S. Clifford, J. Cioslowski, B. Stefanov, G. Liu, A. Liashenko, P. Piskorz, I. Komaromi, R.L. Martin, D.J. Fox, T. Keith, M.A. Al-Laham, C.Y. Peng, A. Nanayakkara, M. Challacombe, P.M.W. Gill, B. Johnson, W. Chen, M.W. Wong, C. Gonzalez, J.A. Pople, Gaussian 09 (now Gaussian 16), Gaussian Inc., Wallingford (CT) 2016.

[16] G. Keresztury, S. Holly, G. Besenyei, J. Varga, A. Wang, J.R. Durig, *Spectrochim. Acta A* **49**, 2007 (1993).

[17] G. Keresztury, in: *Raman Spectroscopy Theory in Handbook of Vibrational Spectroscopy*, Eds. J.M. Chalmers, P.R. Griffith, Wiley, New York 2002.

[18] V. Krishnakumar, R.J. Xavier, *Indian J. Pure Appl. Phys.* **41**, 597 (2003).

[19] P.L. Praveen, D.P. Ojha, *Liq. Cryst.* **41**, 872 (2014).

[20] K. Govindarasu, E. Kavitha, *Spectrochim. Acta A* **133**, 799 (2014).

[21] D.M. Burland, R.D. Miller, C.A. Walsh, *Chem. Rev.* **94**, 31 (1994).

[22] V.M. Geskin, C. Lamber, J.L. Bredas, *J. Am. Chem. Soc.* **125**, 15651 (2003).

[23] D.A. Kleinman, *Phys. Rev.* **126**, 1977 (1962).

[24] A. Ferrarini, G.R. Luckhurst, P.L. Nordio, *Mol. Phys.* **85**, 131 (1995).